Journal of Applied Polymer Science

Effect of Epoxidized Natural Rubber on the Properties of Rectorite/Carbon Black/Natural Rubber Nanocomposites

Lei Wang, Pu-Yu Xiang, Li-Qun Zhang, You-Ping Wu
The State Key Laboratory of Organic-Inorganic Composites, The Key Laboratory of Beijing City on Preparation and Processing of Novel Polymer Materials, Beijing University of Chemical Technology, Beijing 100029, China
Correspondence to: Y.-P. Wu (E-mail: wuyp@mail.buct.edu.cn)

ABSTRACT: Epoxidized natural rubber (ENR) was introduced into rectorite (REC)/carbon black/natural rubber (NR) nanocomposites by two ways: (1) the direct incorporation of ENR and (b) the incorporation of a spray-dried REC/ENR compound. Transmission electron microscopy and X-ray diffraction analysis showed that the REC layers presented a nanodispersion structure in the REC/ENR compound. The vulcanization characteristics indicated that ENR increased the crosslinking density of the composites. The stronger reaction between the REC layers and ENR was verified by Fourier transform infrared spectroscopy in the spray-dried REC/ENR compound blended with NR versus that in the REC/NR master batch blended with ENR. As a result, the physical properties, such as the mechanical properties, cutting and chipping resistance, and abrasion resistance, of the composites were greatly increased by the addition of the REC/ENR compound. © 2012 Wiley Periodicals, Inc. J. Appl. Polym. Sci. 128: 2578–2584, 2013

KEYWORDS: clay; compatibilization; properties and characterization; rubber

Received 22 June 2012; accepted 8 September 2012; published online 26 November 2012
DOI: 10.1002/app.38574

INTRODUCTION

As a reinforcing filler of rubber composites, layered silicates have been widely studied in recent years.[1–5] Compared with the spherical filler carbon black (CB), the layered silicates with their lamellar structure can more effectively inhibit the propagation of cracks in rubber composites.[6–8] Some researchers have investigated the combined effect of CB and layered silicates on the properties of natural rubber (NR) composites.[9–12]

By a latex compounding method (LCM), layered silicates can be dispersed in the rubber matrix on nanometer level.[13–15] Because a pristine layered silicate is used, the interfacial interaction is poor; this hinders further improvement in the physical properties of the composites.[16,17] It has been reported that epoxidized natural rubber (ENR) can be used as a good compatibilizer of clay and the NR matrix; this brings about better reinforcement of NR composites.[18–20]

Rectorite (REC) is an interstratified layered silicate mineral consisting of a regular stacking of micalike layers and montmorillonite-like layers (1:1).[21] A schematic representation of the REC structure[22] is given in Figure 1. The interlayer cations of montmorillonite-like layers can be exchanged easily by either organic or inorganic cations, and therefore, similar to montmorillonite, REC also has water-swelling properties. This makes it possible to prepare REC/rubber nanocompounds by the LCM.

In this study, we intended to compare the effects of ENR on the physical properties of REC/CB/NR nanocomposites by two methods of introducing ENR. In one, ENR was directly added, and accordingly, an REC/NR master batch was prepared by the LCM. In the other, a spray-dried REC/ENR compound was used. The properties of the nanocomposites, such as the curing characteristics, mechanical properties, dynamic viscoelasticity, cutting and chipping resistance (CCR), and abrasion resistance, were investigated in detail. We found that the addition of ENR greatly increased the interfacial interaction between REC and the rubber matrix and the crosslink density; this led to dramatically improved properties in the REC/CB/NR nanocomposites, particularly in the nanocomposite containing the spray-dried REC/ENR compound. These results are expected to provide deep insight into the effects of ENR on layered silicate/rubber nanocomposites.

EXPERIMENTAL

Materials

NR (SCR-1) was purchased from Yunnan State Farm Group Co., Ltd. (Kunming, China). NR latex (solid content = 61%) was supplied by Beijing Latex Products Factory (Beijing, China). Commercial-grade solid ENR and ENR latex having 50 mol % epoxy groups (ENR50, solid content of latex = 31%) were purchased from the Chinese Academy of Tropical Agricultural Science (Zhanjiang, China). The glass-transition temperatures of

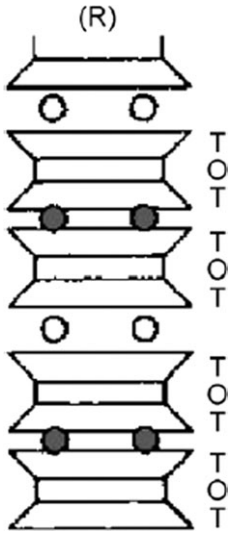

Figure 1. Schematic representation of the REC structure.[22] The TOT three-layer sequence is represented by trapezoids and rectangles, where T is the tetrahedral sheet and O is the octahedral sheet. Exchangeable and nonexchangeable charge-compensating cations are represented by open and solid circles, respectively.

NR and ENR50, as measured by differential scanning calorimetry experiments, were −66 and −13°C, respectively. CB (N330) was from Tianjin Dolphin Carbon Black Co., Ltd. (Tianjin, China). REC, with a cation-exchange capacity of 44.9 mequiv/100 g, was purchased from Hubei Celebrities Rectorite Technology Co., Ltd. (Zhongxiang, China). Other products used were commercially available.

Preparation of the REC/ENR Compound

First, REC was dispersed in deionized water with vigorous stirring, and an aqueous suspension of REC with a solid content of 1.3 wt % was obtained. Then, a given amount of ENR latex was added to the aqueous suspension, and the mixture was stirred for 30 min. Finally, the mixture was spray-dried into the REC/ENR compound (REC/ENR mass ratio = 1:3). The processing parameters of spray drying were as follows: the inlet and outlet air temperatures were 220 and 100°C, respectively; the feeding rate was 400 mL/h; and the air pressure was 0.46 MPa.

Preparation of the REC/NR Master Batch

The REC/NR master batch (REC/NR mass ratio = 1:5) was prepared by LCM.[23] A given amount of NR latex was added to the aqueous suspension of REC, and the mixture was stirred for 30 min. After that, the mixture was cocoagulated in an about 1 wt % sulfuric acid solution, washed with water until it was neutral, and then dried in an oven at 50°C for 20 h to obtain the REC/NR master batch.

Preparation of the REC/CB/NR Nanocomposites

The basic formulas are listed in Table I. ENR [12 parts per hundred rubber (phr)] was introduced by the direct addition of ENR or the blending of the REC/ENR compound. Accordingly, REC was introduced via an REC/NR master batch or an REC/ENR compound, respectively. Three samples are examined herein, A1, A2, and A3, and the loading of REC was 4 phr in the three formulas. A1, as a reference, was the composite containing a 24-phr REC/NR master batch without ENR. In A2, 12 phr ENR, instead of the same amount of NR, was incorporated as the compatibilizer; whereas in A3, a 16-phr REC/ENR compound containing 4 phr REC was employed. According to Table I, the NR, REC/NR master batch, REC/ENR compound, CB, and other ingredients were mixed uniformly on a 6-in., two-roll mill (Zhanjiang Rubber & Plastic Machine Factory, Zhanjiang, China) at room temperature. Then, the compounds were vulcanized (Shanghai Rubber Machine Factory, Shanghai, China) at 150°C for the optimum cure time (t_{90}) in a standard mold to produce the REC/CB/NR nanocomposites.

Characterization

X-Ray Diffraction (XRD) Analysis. XRD analyses of the REC/ENR compound and REC/NR master batch were carried out on a 2500VB2+PC diffractometer (Rigaku, Tokyo-to, Japan) with Cu Kα radiation (40 kV and 50 mA) at a scanning rate of 1°/min from 1 to 10°.

Transmission Electron Microscopy (TEM). The samples of the REC/ENR compound, REC/NR master batch, and REC/CB/NR nanocomposites for TEM observation were ultrathin sections prepared by a cryoultramicrotome. The REC/ENR compound and REC/NR master batch were shaped into sheets on the two-roll mill before sample preparation. TEM micrographs were taken with an H-800 TEM instrument (Hitachi, Tokyo, Japan) at an acceleration voltage of 200 kV.

Fourier Transform Infrared (FTIR) Spectroscopy. To characterize and compare the reaction between REC and ENR in A2 and A3 during the curing process, REC/ENR/NR compounds with a mass ratio of 1:3:5 were prepared by two different methods: (1) the REC/ENR compound was melt-blended with NR, and (2) the REC/NR master batch was melt-blended with ENR. Then, the two REC/ENR/NR compounds were treated at 150°C for 10.2 min (t_{90} of A2) in a standard mold before testing. We shaped the pill-like sample of REC, as a reference, by maintaining the powder in a tablet compression machine (Tianjin

Table I. Basic Formulas of the REC/CB/NR Nanocomposites

Sample	A1	A2	A3
NR	80	68	88
ENR		12	
REC/NR master batch	24	24	
REC/ENR compound			16
CB	50	50	50
Zinc oxide	5	5	5
Stearic acid	2	2	2
Antioxidant 4010NA[a]	0.5	0.5	0.5
Wax	1	1	1
Accelerator DM[b]	1.8	1.8	1.8
Aromatic oil	6	6	6
Sulfur	1.4	1.4	1.4

[a]Antioxidant 4010NA: *N*-isopropyl-*N*′-phenyl-*p*-phenylenediamine.
[b]Accelerator DM: dibenzothiazole disulfide.

Applied Polymer SCIENCE

Tianguang Optic Machine Co., Ltd., Tianjin, China) under 20 MPa of pressure for 15 min at room temperature.

FTIR spectra of the three previous samples were obtained from an accumulation of 32 scans at a resolution of 4 cm^{-1} in the attenuated total reflection mode with a TENSOR27 FTIR spectrometer (Bruker Optic Gmbh, Ettlingen, Germany) at ambient temperature.

Test of the Dynamic Viscoelastic Properties. Strain sweep experiments of the uncured REC/CB/NR nanocompounds were performed with an RPA 2000 rubber process analyzer (Alpha Technologies, Akron, Ohio, USA) in a strain range of 0.28–400% at 100°C and 1 Hz. For the cured REC/CB/NR nanocomposites, the test conditions of the strain sweep experiments performed with rubber process analysis (RPA) were 0.28–40% at 60°C and 10 Hz.

The dynamic mechanical properties of the REC/CB/NR nanocomposites were measured with a dynamic mechanical thermal analyzer (VISCOANALYSEUR VA 3000, 01dBMetravib Co., Ltd., Rhone, France) in tension mode with dimensions of 20 × 15 × 2 mm^3 at a frequency of 10 Hz with a strain amplitude of 0.1%; the temperature was increased at 3°C/min from −80 to 80°C.

Mechanics Performance Test. The mechanical properties were measured according to ASTM D 412 with a CMT 4104 electrical tensile tester (Shenzhen Sansi Zongheng Technology Co., Ltd., Shenzhen, China) at a speed of 500 mm/min. An XY-1 rubber hardness apparatus (4th Chemical Industry Machine Factory, Shanghai, China) was used to measure the hardness (Shore A) according to ASTM D 2240-75.

CCR Test. The CCR test of the composites was performed with a BF Goodrich Cut and Chip Tester (Beijing Wanhui Yifang Science and Technology Development Co., Ltd., Beijing, China). For the CCR test, the specimen was rolled at a speed of 720 cycles/min for 20 min, and the cutting frequency was 2 Hz. CCR for the composite was determined by the average mass loss of the three specimens.

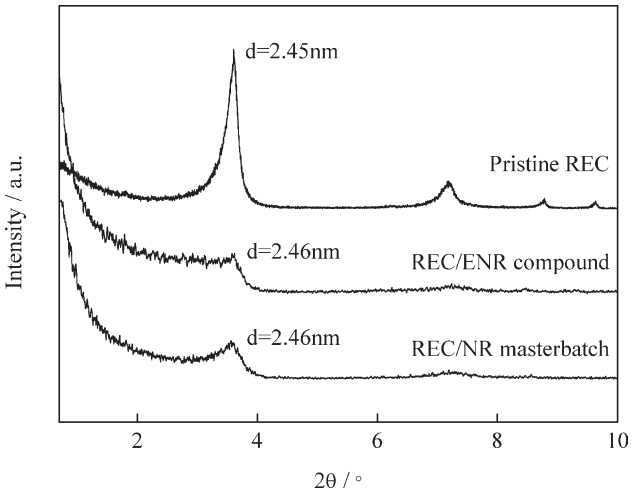

Figure 2. XRD patterns of the pristine REC, the REC/ENR compound with a mass ratio of 1:3, and the REC/NR master batch with a mass ratio of 1:5.

Akron Abrasion Test. The Akron abrasion of the composites was tested by an abrasion machine (MZ-4061, Mingzhu Experimental Machinery Co., Ltd., Jiangdu, China). The specimen was adhered onto a rubber wheel. For the abrasion test, the specimen was rolled against a grinding wheel for 800 cycles (0.38 km) to remove the fresh surface and then rolled for 1.61 km. The volume loss during the 1.61-km rolling was regarded as the Akron abrasion loss.

RESULTS AND DISCUSSION

Structure and Morphology of the REC/ENR Compound and REC/NR Master Batch

The XRD patterns of the REC/ENR compound and REC/NR master batch are presented in Figure 2. A peak corresponding to a layer spacing of 2.45 nm appeared in the spectra of the pristine REC, which is the diffraction peak of the (001) lattice plane of REC.[24] For the REC/ENR compound and REC/NR master batch, the curves were very similar, and the peak of REC

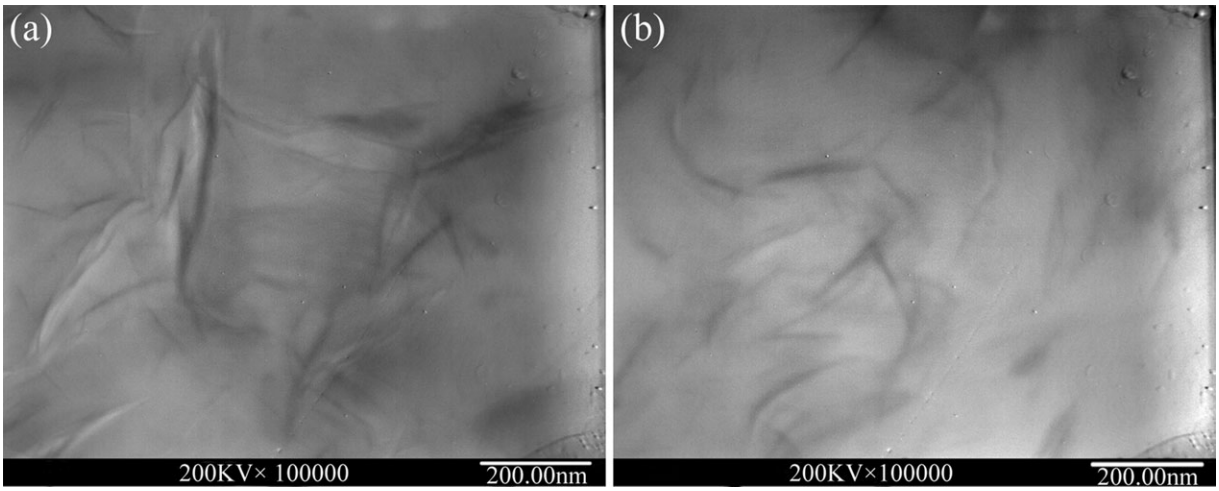

Figure 3. TEM photos of (a) the REC/ENR compound with a mass ratio of 1:3 and (b) REC/NR master batch with a mass ratio of 1:5.

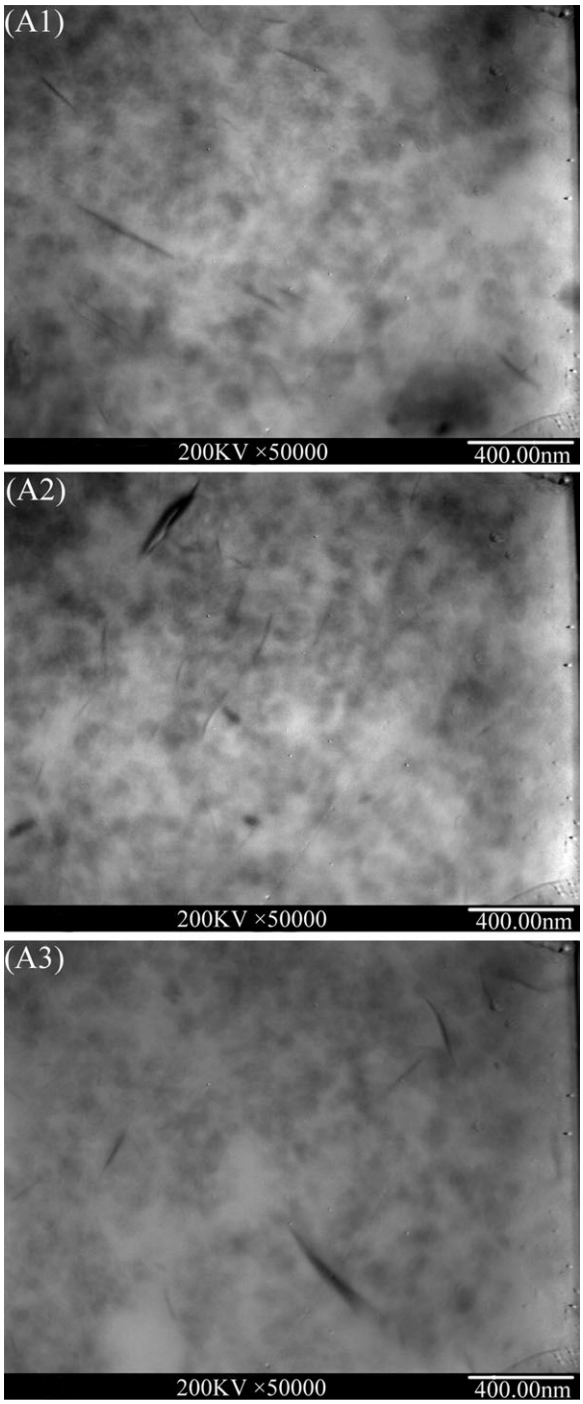

Figure 4. TEM photos of the REC/CB/NR nanocomposites.

(d_{001} = 2.46 nm) still existed, but the peak intensity decreased. This indicated that there were also some stacking layers without rubber macromolecules intercalated therein,[23] and some REC layers were exfoliated; this resulted in an obvious decrease in the peak intensity. That is, both the spray-dried REC/ENR compound and REC/NR master batch prepared by the LCM exhibited a separated structure:[15] ENR or NR macromolecules isolated the REC layers into single layers and stacking layers on the nanometer level in the preparation process.

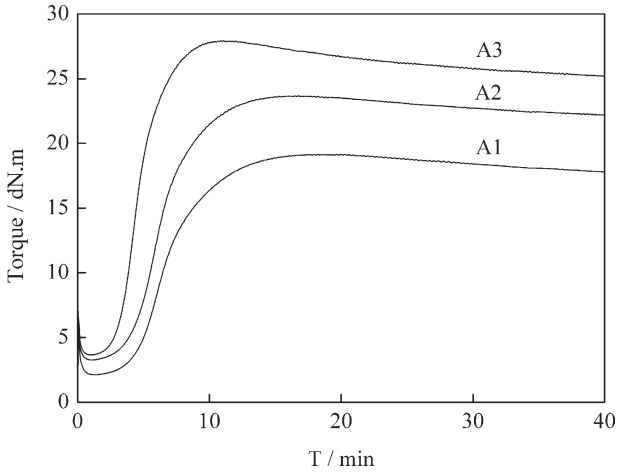

Figure 5. Vulcanization curves of the REC/CB/NR nanocomposites (T = time).

To acquire more information about the morphology of the REC/ENR compound and REC/NR master batch, we obtained TEM micrographs, as presented in Figure 3. As shown in Figure 3, the REC layers presented a nanodispersion structure in both the ENR and NR matrices, and single REC layers and stacking REC layers coexisted. This was consistent with the results of XRD. As also shown in Figure 3, the number of REC layers in the REC/ENR compound was much greater than that in the REC/NR master batch; this was due to the higher mass ratio of REC to ENR (1:3) than that of REC to NR (1:5). The previous results indicate that the spray-drying method is effective to ensure the nanodispersion of REC layers.

Morphology of the REC/CB/NR Nanocomposites

To investigate the dispersion of fillers, we obtained TEM micrographs of the REC/CB/NR nanocomposites, as shown in Figure 4. The dark lines are the intersections of the REC layers. In the three composites, the REC layers also presented a nanodispersion structure similar to the dispersion in the REC/ENR compound and REC/NR master batch

Vulcanization Characteristics of the REC/CB/NR Nanocomposites

The vulcanization characteristics of the REC/CB/NR nanocomposites are presented in Figure 5 and Table II. Compared with A1, the t_{90} values of A2 and A3 were reduced, especially for A3; this demonstrated that the vulcanization of the composites was accelerated by ENR. As shown in Table II, the difference (ΔM) between

Table II. Vulcanization Characteristics of the REC/CB/NR Nanocomposites

Sample	A1	A2	A3
t_{90} (min)	11.4	10.2	7.2
M_L (dN m)	2.12	3.25	3.65
M_H (dN m)	19.15	23.67	27.72
ΔM (dN m)	17.03	20.42	24.07

Applied Polymer SCIENCE

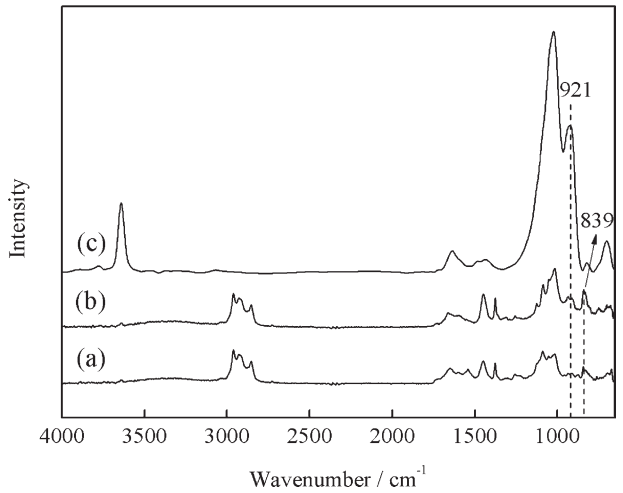

Figure 6. FTIR spectra of the REC/ENR/NR compounds by two different methods: (a) the REC/ENR compound melt-blended with NR, (b) the REC/NR master batch melt-blended with ENR, and (c) pristine REC.

the minimum torque (M_L) and the maximum torque (M_H) increased when ENR was introduced into the nanocomposites; this implied an increase in the crosslink density. Both the reduced curing time and the increased crosslink density could be explained by the activation of adjacent double bonds by the epoxy group.[25] It is worth noticing that despite the same composition, the crosslink density of A3 was higher than that of A2. This may be explained as follows: in A3, the REC/ENR compound was used, the surface of the REC layers was covered by ENR molecules, and the epoxy group could interact with the hydroxyl on the surface of the REC layers. Thus, the interaction between the OH groups on the REC surface and the curing agents could be effectively avoided.[20] This led to the higher crosslink density.

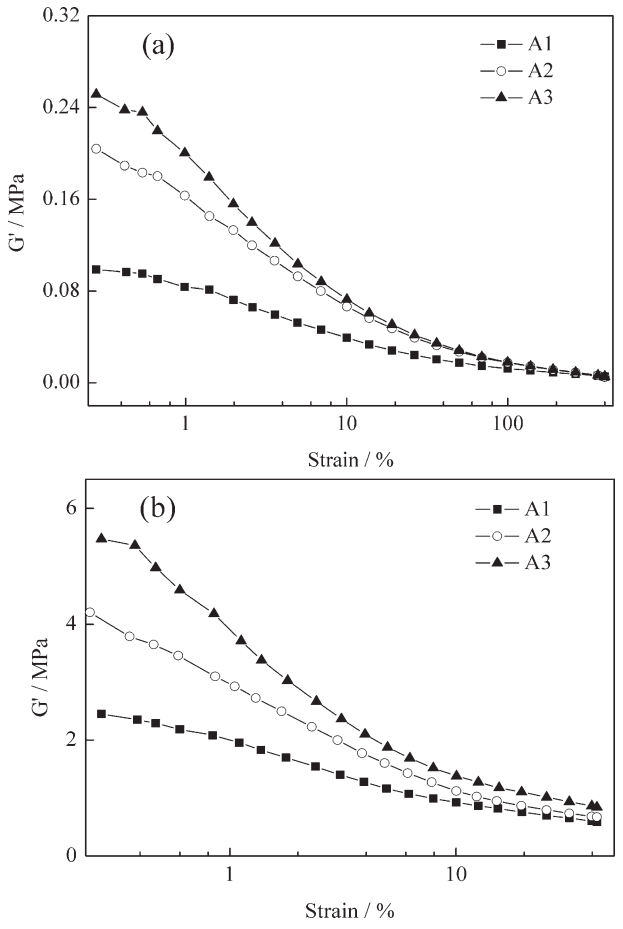

Figure 7. Storage modulus (G') versus strain curves of the REC/CB/NR (a) nanocompounds and (b) nanocomposites measured by RPA.

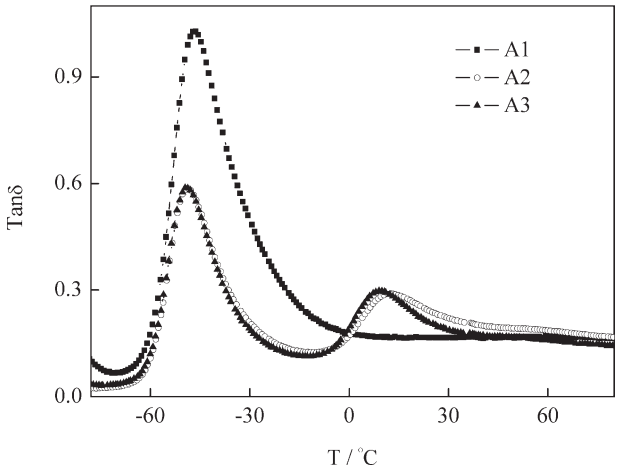

Figure 8. Loss factor versus temperature curves of the REC/CB/NR nanocomposites measured by DMTA (T = temperature).

As shown in Figure 5, ENR improved the M_L and M_H values, that is, the viscosity and modulus of composites,[18,26] of A2 and A3; this was in agreement with the results of other researchers.[27,28] Compared with those of A2, the viscosity and modulus of A3 were further enhanced; this might have resulted from the stronger reaction between the ENR and REC layers in A3. To confirm this assumption, we conducted FTIR analysis of the REC/ENR/NR compounds prepared by two different methods, as discussed next.

FTIR Analysis of the Reaction between REC and ENR

The FTIR spectra of the two REC/ENR/NR compounds prepared by two different methods are presented in Figure 6. From Figure 6, the peak at 921 cm^{-1}, which was attributed to the Al—OH liberation of REC,[29] was observed in the spectra of the pristine REC. The intensity of the peak at 921 cm^{-1} decreased in the two REC/ENR/NR compounds. Particularly, in the spray-dried REC/ENR compound melt-blended with NR, the peak almost disappeared. In addition, the peak at 839 cm^{-1} of epoxy stretching[30] was also attenuated in the spray-dried REC/ENR compound melt-blended with NR. Therefore, the reaction between the hydroxyl groups on the REC surface and the epoxy groups in ENR was stronger in the spray-dried REC/ENR compound blended with NR than in REC/NR master batch blended with ENR. The results show direct evidence to explain the curing curves of A2 and A3.

Dynamic Viscoelastic Properties of the REC/CB/NR Nanocomposites

To investigate the effect of ENR on the dynamic viscoelastic properties, the strain sweep curves of the REC/CB/NR

Table III. Mechanical Properties of the REC/CB/NR Nanocomposites

Sample	A1	A2	A3
Shore A hardness (°)	61	65	69
Stress at 100% (MPa)	2.0	2.9	3.5
Stress at 300% (MPa)	8.3	10.7	12.0
Tensile strength (MPa)	22.1	24.9	29.7
Elongation at break (%)	545	556	560
Tear strength (kN/m)	77.8	84.1	96.2

nanocompounds measured by RPA are shown in Figure 7(a). Figure 7(a) shows that the order of the initial modulus values was A3 > A2 > A1; this resulted from the higher viscosity of ENR itself and, more importantly, the stronger interfacial interaction between the REC layers and ENR in A3. After curing, the difference between the curves of A2 and A3 was amplified [Figure 7(b)] by the higher crosslink density of A3 compared to that of A2, as discussed previously.

Figure 8 presents curves of the loss factor (tan δ) as a function of the temperature in the range −80 to 80°C, as measured by dynamic mechanical thermal analysis (DMTA). In Figure 8, the two peaks in the curves of A2 and A3 correspond to the glass-transition peaks of NR and ENR, respectively. Moreover, compared with those of A2, the two peaks in A3 came closer to each other; this demonstrated that REC promoted the compatibility between ENR and NR, as reported by other researchers.[20]

Mechanical Properties of the REC/CB/NR Nanocomposites

The mechanical properties of the REC/CB/NR nanocomposites are presented in Table III. As shown in Table III, compared with those of A1, the hardness, stresses at 100 and 300%, and the tensile and tear strengths of A2 and A3 were dramatically increased through the addition of ENR, particularly for A3. This was attributed to the higher crosslink density[31] and stronger interfacial interaction between the ENR and REC layers, as discussed previously.

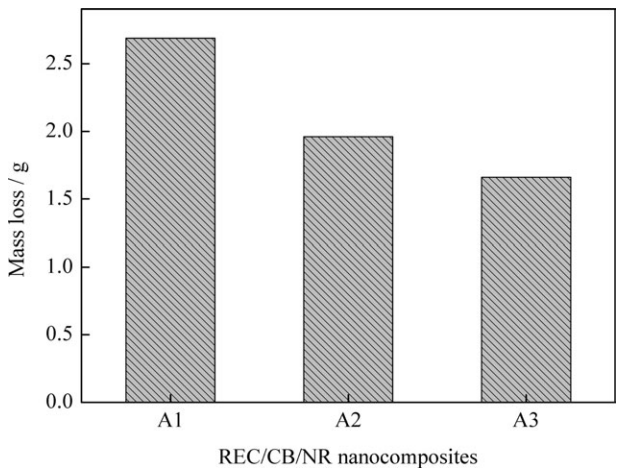

Figure 9. Cutting mass loss of the REC/CB/NR nanocomposites.

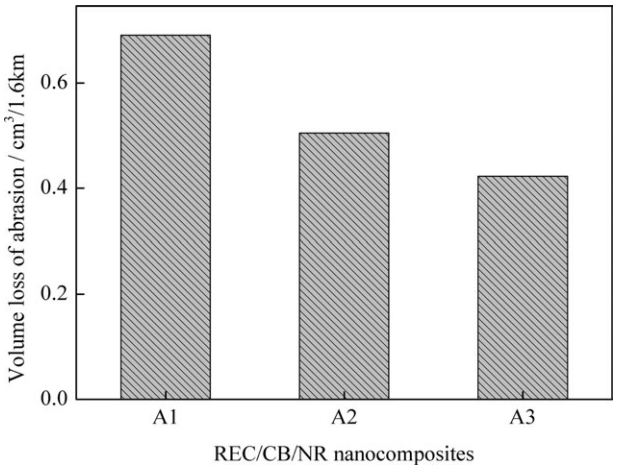

Figure 10. Volume loss of the abrasion loss of the REC/CB/NR nanocomposites.

CCR of the REC/CB/NR Nanocomposites

The cutting mass loss of the REC/CB/NR nanocomposites is presented in Figure 9. From Figure 9, the cutting mass loss of the composites was obviously reduced after ENR was added; this indicated that the CCR was considerably improved. In fact, the CCR test was a repeated-impact process, in which the microcrack occurred on the surface of samples; then, the microcrack was propagated further by the repeated impact, and finally, the debris was detached from the composites.[8] As can be seen in Table III, the mechanical properties of the composites were greatly improved in A2 and A3. This implied that the resistance to damage of the composites was dramatically increased. This could have contributed to the increase in the CCR of the composites.

Abrasion Resistance of the REC/CB/NR Nanocomposites

Figure 10 displays the Akron abrasion resistance of the REC/CB/NR nanocomposites. As shown in Figure 10, A2 and A3 exhibited much better abrasion resistances than A1. The abrasion resistance of the composites was closely related to the interfacial interaction between the filler and the rubber.[32] With addition of ENR to A2 and A3, the interfacial interaction was enhanced, especially in A3. Apart from the interfacial interaction, the mechanical properties of the rubber composites bore a relation to the abrasion resistance as well.[33] Therefore, the abrasion resistance of A2 and A3 were greatly increased by the improved interfacial interaction and mechanical properties, particularly for A3.

CONCLUSIONS

The REC layers presented a highly dispersed structure in the spray-dried REC/ENR compound. ENR increased both the crosslinking density of the composites and the interfacial interaction between the REC layers and the rubber matrix, particularly for the composite filled with the REC/ENR compound. As a result, the physical properties of the composites, such as the mechanical properties, CCR, and abrasion resistance, were greatly improved accordingly by the addition of the REC/ENR compound.

ACKNOWLEDGMENTS

The authors thank the Program for New Century Excellent Talents in University (contract grant number NCET-10-0202) and the National Natural Science Foundation of China (contract grant number 51073009) for financial support.

REFERENCES

1. Wu, Y. P.; Jia, Q. X.; Yu, D. S.; Zhang, L. Q. *J. Appl. Polym. Sci.* **2003**, *89*, 3855.
2. Wu, Y. P.; Ma, Y.; Wang, Y. Q.; Zhang, L. Q. *Macromol. Mater. Eng.* **2004**, *289*, 890.
3. Ma, Y.; Wu, Y. P.; Wang, Y. Q.; Zhang, L. Q. *J. Appl. Polym. Sci.* **2006**, *99*, 914.
4. Hrachová, J.; Komadel, P.; Chodá, K. I. *J. Mater. Sci.* **2008**, *43*, 2012.
5. Kaneko, M. L. Q. A.; Romero, R. B.; Gonçalves, M. D. C.; Yoshida, I. V. P. *Eur. Polym. J.* **2010**, *46*, 881.
6. Wu, Y. P.; Zhao, W.; Zhang, L. Q. *Macromol. Mater. Eng.* **2006**, *291*, 944.
7. Wu, X. H.; Liu, J.; Wang, Y. Q.; He, S. J.; Zhang, L. Q. *Polym. Eng. Sci.* **2012**, *52*, 1027.
8. Ma, J. H.; Wang, Y. X.; Zhang, L. Q.; Wu, Y. P. *J. Appl. Polym. Sci.* **2012**, *125*, 3484.
9. Bhattacharya, M.; Bhowmick, A. K. *J. Mater. Sci.* **2010**, *45*, 6126.
10. Bhattacharya, M.; Bhowmick, A. K. *J. Mater. Sci.* **2010**, *45*, 6139.
11. Jia, Q. X.; Wu, Y. P.; Xiang, P.; Ye, X.; Wang, Y. Q.; Zhang, L. Q. *Polym. Polym. Compos.* **2005**, *13*, 709.
12. Qu, L. L.; Huang, G. S.; Zhang.P.; Nie, Y. J.; Weng, G. S.; Wu, J. R. *Polym. Int.* **2010**, *59*, 1397.
13. Zhang, L. Q.; Wang, Y. Z.; Wang, Y. Q.; Sui, Y.; Yu, D. S. *J. Appl. Polym. Sci.* **2000**, *78*, 1873.
14. Varghese, S.; Karger-Kocsis, J. *Polymer* **2003**, *44*, 4921.
15. Wu, Y. P.; Wang, Y. Q.; Zhang, H. F.; Wang, Y. Z.; Yu, D. S.; Zhang, L. Q.; Yang, J. *Compos. Sci. Technol.* **2005**, *65*, 1195.
16. Jia, Q. X.; Wu, Y. P.; Wang, Y. Q.; Lu, M.; Yang, J.; Zhang, L. Q. *J. Appl. Polym. Sci.* **2007**, *103*, 1826.
17. Jia, Q. X.; Wu, Y. P.; Wang, Y. Q.; Lu, M.; Zhang, L. Q. *Compos. Sci. Technol.* **2008**, *68*, 1050.
18. Teh, P. L., Mohd Ishak, Z. A.; Hashim, A. S.; Karger-Kocsis, J.; Ishiaku, U. S. *Eur. Polym. J.* **2004**, *40*, 2513.
19. Pal, K.; Rajasekar, R.; Kang, D. J.; Zhang, Z. X.; Kim, J. K.; Das, C. K. *Mater. Des.* **2009**, *30*, 4035.
20. Arroyo, M.; López-Manchado, M. A.; Valentín, J. L.; Carretero, J. *Compos. Sci. Technol.* **2007**, *67*, 1330.
21. Yao, Q.; Wang, C. X.; Zhao, L. Q. *Mineral. Res. Geolog.* **2001**, *15*, 264.
22. Olivier, J. P.; Occelli, M. L. *Micropor. Mesopor. Mat.* **2003**, *57*, 291.
23. Wang, Y. Q.; Zhang, H. F.; Wu, Y. P.; Yang, J.; Zhang, L. Q. *Eur. Polym. J.* **2005**, *41*, 2776.
24. Xiao, J. R.; Peng, T. Y.; Dai, K.; Zan, L.; Peng, Z. H. J. *Solid State Chem.* **2007**, *180*, 3188.
25. Poh, B. T.; Tan, B. K. *J. Appl. Polym. Sci.* **1991**, *42*, 1407.
26. Carli, L. N.; Roncato, C. R.; Zanchet, A.; Mauler, R. S.; Giovanela, M.; Brandalise, R. N.; Crespo, J. S. *Appl. Clay Sci.* **2011**, *52*, 56.
27. Ismail, H.; Leong, H. C. *Polym. Test.* **2001**, *20*, 509.
28. Fernandes, R. M. B.; Visconte, L. L. Y.; Nunes, R. C. R. *Int. J. Polym. Mater.* **2011**, *60*, 351.
29. Li, Z. H.; Jiang, W. T.; Hong, H. L. *Spectrochim. Acta A* **2008**, *71*, 1525.
30. Ratnam, C. T.; Nasir, M.; Baharin, A.; Zaman, K. *Polym. Degrad. Stab.* **2001**, *72*, 147.
31. Zhao, F.; Bi, W. N.; Zhao, S. G. *J. Macromol. Sci. B* **2011**, *50*, 1460.
32. Findik, F.; Yilmaz, R.; Köksal, T. *Mater. Des.* **2004**, *25*, 269.
33. Mathew, L.; Joseph, R. *J. Appl. Polym. Sci.* **2007**, *103*, 1640.